ELSEVIER

International Journal of Mass Spectrometry 200 (2000) 313–330

International Journal of Mass Spectrometry

Gas phase ion thermochemistry based on ion-equilibria From the ionosphere to the reactive centers of enzymes

Paul Kebarle*

Department of Chemistry, University of Alberta, Edmonton, AB, Canada T6G 2G2

Received 12 June 2000; accepted 17 August 2000

Abstract

The discovery that ion-molecule equilibria can be determined in the gas phase with mass spectrometers, which was made accidentally with a high-pressure mass spectrometer constructed for other purposes, has led to the development of a vast field of gas-phase ion-equilibria determinations with mass spectrometers. Data have been obtained for many thousands of important reactions, such as the ion-solvent molecule and ion-ligand bonding interactions, basicities of bases B and acidities of acids AH in the gas phase, stabilities of carbocations, and electron affinities of molecules. The data have applications in many areas of chemistry. Examples of such applications are given. (Int J Mass Spectrom 200 (2000) 313–330) © 2000 Elsevier Science B.V.

Keywords: Ion energetics; Ion solvation; Ion-ligand bond energies; Proton affinity; Electron affinity; Hydride ion affinity; Gas phase acidity

1. Introduction

Results from measurements of ion equilibria in solution, compiled in the form of acid–base dissociation constants, stability constants for ion–ligand complexes and electrochemical oxidation-reduction potentials, represent the quantitative backbone of chemistry in solution. Such measurements began in the early 1900s, and at the present this material is a major part of first-year college chemistry, and the data are used in all branches of chemistry. Notable also is the use of equilibrium data in modern biochemistry, such as determination of the stability of Zn^{2+} ions inside metalloenzymes like carbonic anhydrase and carboxypeptidase, relative to the surrounding aqueous phase of the cytoplasm [1] and determinations of the stability constants of protein-substrate complexes [2].

The same type of fundamental reactions—proton transfer, ion-ligand association, ion-solvent molecule(s) association, electron transfer—occur also in the gas phase. Obviously reliable information based on determination of such equilibria in the gas phase was potentially available and the instrument with which to observe such reactions was most likely a modified mass spectrometer. However, the work in our laboratory, which started in 1962 and led, between 1962 and 1970, to the development of mass spectrometric methods with which such equilibria could be determined [3–17], did not originate from a deliberate attempt to develop such an instrument and engage in ion-equilibria studies. The occurrence of equilibria was observed accidentally, when performing experiments under unusual conditions.

Radiation chemistry was an important research area in the years after World War II (i.e. in the 1950s and 1960s). The effects of ionizing radiation were very much brought to the fore by the development of

*Corresponding author.
E-mail: paul.kebarle@ualberta.ca

PII S1387-3806(00)00326-2

nuclear weapons. The ionic part of the reactions induced by ionizing radiation in gases was amenable to mass spectrometric investigation. The first investigations of ion-molecule reactions, with more or less conventional low-pressure mass spectrometers by Talroze and Lubimova [18], Stevenson and Schissler [19], and Field et al. [20] were at least in part inspired by the interest in radiation chemistry.

To achieve abundant ion-molecule collisions and reactions, the ion sources were gradually operated at higher and higher pressures. At pressures of 1 Torr, abundant ion molecule reactions were observed. However, conventional radiation chemistry of gases was studied at 1 atm and there were reasons to believe that at such high pressures the outcome of the ion-molecule reactions may be different [3]. For this reason my first postdoctoral fellow, Nata Godbole, and I decided, probably in 1962, to try to observe mass spectrometrically ion-molecule reactions at 1 atm or near 1 atm.

Three modifications of conventional mass spectrometers were required to achieve this task: (a) reduce the outflow from the ion source-reaction chamber, by making the ion exit orifice very small; (b) increase the pumping speed outside the ion source; (c) increase the penetrating power of the ionizing medium. The first two changes had been applied by the previous workers [8–10], but not radically enough. For example, the pumping speed had been increased to 10 L/s, whereas close to 1000 L/s were required at 1 atm. I ordered the necessary large diffusion pumps and gave the drawings for the associated pumping system to the Chemistry Department's Machine Shop. As a penetrating ionization medium we chose a polonium α-particle source [4]. Fortunately, at that time, we could get funding directly from the University of Alberta, and no proposal was required. Because the project was essentially a step into the unknown, I doubt that it would have been undertaken had a formal proposal been necessary. The mass spectrometer used was the one and only instrument in the Department, a 90° magnetic sector that had been homemade at the Canadian National Research Council (NRC) and that I had assembled in Edmonton with help from my former postdoctoral supervisor, Fred Lossing of NRC.

The first experiments at near-atmospheric pressure, between 300 and 10 Torr led to mass spectra that were very hard to interpret [4]. When a single gas was introduced, such as nitrogen, oxygen or argon, we did not see any ions that could be attributed to the gas used (i.e., no N_2^+ ions were observed with N_2, no O_2^+) ions with O_2, and so on. One observation that became significant was the presence of ion groups whose mass differed by 18 units. Of great help was the report by Knewstubb and Tickner [21] of the mass spectrometric observation of $H_3O^+(H_2O)_n$ ions in electric gas discharges at low pressures. Our ions seldom had H_3O^+ as the core ion. Core ions of all kinds of possible masses occurred when the above pure gases were used.

It took us some time to realize that even though water vapor was the major impurity in the gases used, and therefore hydrates $X^+(H_2O)_n$ were observed, other impurities present at much lower levels (parts per million) determined the nature of the observed core ion. The picture became clearer after we worked [5] with some neat gases with high gas-phase basicities such as NH_3, which led to core ions that were predominantly NH_4^+ and clusters of $NH_4^+(NH_3)_n$.

To avoid mass spectra dominated by unknown trace impurities, the major gases used had to be extremely pure and the gas-handling systems had to be of ultrahigh vacuum quality (i.e. of glass and metal only) so as not to retain previously used compounds. When such changes were made, the ions observed became more predictable. Thus $H_3O^+(H_2O)_n$ ions were observed with water vapor in the ion source and not $X^+(H_2O)_n$ due to some unknown trace impurity B with high proton affinity which rapidly took the proton away from H_3O^+ and led to $BH^+ = X^+$.

Observations [5–7] of the mass spectra $NH_4^+(NH_3)_n$ with neat NH_3 and $H_3O^+(H_2O)_n$ with neat H_2O vapor, at increasing pressure of the solvent vapor and at different ion source temperatures indicated that ion-molecule equilibria were present. Thus, at constant temperature when the solvent S pressure was increased, a shift of the intensities to higher n was observed. Increase of ion source temperature at constant pressure led to shifts toward lower n values. Realizing that, if equilibria really did occur, their determinations would lead to far more important results than the radiation chemistry investigations, we

concentrated fully on developing conditions for equilibria measurements. If equilibria were present, the ion intensities I_n should obey the equilibrium equations, that is, for the ion BH^+ solvent molecule S association reactions (1):

$$BH^+S_{n-1} + S = BH^+S_n \qquad (n-1, n) \qquad (1)$$

$$K_{n-1,n} = \frac{I_n}{I_{n-1}\, P_L} \qquad (2)$$

the equilibrium constant expression Eq. (2) should be obeyed and experiments showed that this was the case.

The equilibrium constants $K_{n-1,n}$ could then be used to obtain the free energy change $\Delta G^\circ_{n-1,n}$:

$$-\Delta G^\circ_{n-1,n} = RT \ln K_{n-1,n} \qquad (3)$$

$$\Delta G^\circ_{n-1,n} = \Delta H^\circ_{n-1,n} - T\Delta S^\circ_{n-1,n} \qquad (4)$$

Determinations of the equilibrium constants at different temperatures T, would lead, via van't Hoft plots, to the enthalpy $\Delta H^\circ_{n-1,n}$ and entropy change $\Delta S^\circ_{n-1,n}$ for the reaction [see Eq. (4)].

Even though relationships like Eq. (2) tended be obeyed, we remained skeptical for some time. The conditions in conventional mass spectrometer ion sources are far removed from thermal equilibrium conditions, so we did not understand why we were able to observe thermal equilibria at high pressures. Understanding came only gradually. The high pressures used slowed down very much the diffusion of the ions to the wall, and this increased greatly the residence time of the ions in the ion source. The ions were trapped in the ion source. The long time available allowed the reaction equilibria to establish. The high-pressure gas was also ideal for thermalizing the ions. The low intensity of ionizing radiation used led to very low ion and electron concentrations so that ion-electron recombination was slower than the ion diffusion to the wall, and this led to simple first-order ion-loss kinetics. Because the reactant S concentrations were high, equilibria as in Eq. (1) established much faster than the ion loss to the wall.

However, this did not solve all the problems. The ion-sampling by bleeding gas and ions out of the reaction chamber to the vacuum of the mass spectrometer might lead to ion-intensity ratios I_n/I_{n-1} [see Eq. (2)] that are not the same as the concentration ratio $[BH^+S_n]/[BH^+S_{n-1}]$ in the ion source reaction chamber. Much effort was also expended to provide the proper sampling conditions [4–7]. For a discussion of the sampling conditions and other experimental details concerning the apparatus and method, see Ref. [22].

Another reassurance that equilibria were present and were being determined, came from the actual thermochemical values that were obtained [7,8]. The magnitudes of the $\Delta H^\circ_{n-1,n}$ and $\Delta S^\circ_{n-1,n}$ values obtained were of the right magnitude. Actually, there were very few data available in the literature with which to compare the results. The first extensive study [8] that provided $\Delta G^\circ_{n-1,n}$, $\Delta H^\circ_{n-1,n}$ and $\Delta S^\circ_{n-1,n}$ from $n = 1$ to $n = 7$, was for the very important system:

$$H_3O^+(H_2O)_{n-1} + H_2O = H_3O^+(H_2O)_n \,(n-1,n) \qquad (5)$$

In 1967, there were no theoretical (ab initio) results of any kind, even for the lowest (0,1) changes in this series. The only relevant values with which the equilibrium results for H_3O^+ could be compared were results from an electrostatic calculation for Na^+ and H_2O which led to $\Delta H^\circ_{0,4} = -104$ kcal/mol and $\Delta H^\circ_{0,6} = -115$ kcal/mol. The radius of Na^+ was expected to be similar to the radius of H_3O^+, for which the equilibrium results were $\Delta H^\circ_{0,4} = -91$ kcal/mol, $\Delta H^\circ_{0,6} = -115$ kcal/mol. The approximate agreement between the two sets of data gave us hope that we were in the right ballpark. The entropy changes also appeared to be of the right magnitude. Fortunately, I had taken a course on statistical mechanics as a graduate student at UBC, just because I was interested in the subject. I had understood well the material for ideal gases and ideal solids, but much less well (actually not at all) the treatment of liquids. But now, the knowledge about gases came in handy and we could estimate that the observed large loss of entropy [8], such as $\Delta S^\circ_{0,1} = -33$ cal/(mol · deg), was consistent with the expected large loss of translational entropy in this adduct forming reaction. It has turned out that the ΔG°, $\Delta H^\circ$and ΔS° results [8], were much

better than just "of the right order of magnitude"—they have remained essentially unchanged to the present day.

The realization that very good conditions for determining ion-molecule equilibria existed also at lower total pressures, such as in the 1 − 10 Torr range, allowed the development of simpler apparatus where ionization was obtained with a 1000-V electron beam, which could be pulsed. The introduction of short electron pulses of a few microseconds allowed the observation of the ion-intensity changes due to ion-molecule reactions and ion diffusion to the wall of the ion source, over a few milliseconds between pulses. Thus, not only the equilibria, but also the reaction kinetics leading to the equilibria, could be observed [16,17]. With the development [16,17] of the pulsed high-pressure mass spectrometer (PHPMS), the method had gained great new capabilities. Only small changes in instrumentation and method have occurred since then [22]. Some of the first results with the PHPMS led to an interesting study of ion molecule reactions in the ionosphere, which justify the title of this article. A brief account of these results is given in Section 2.1.

Although the ion-ligand equilibria were the first to be studied [5–15], it soon became clear that other ion-molecule equilibria such as proton transfer, hydride ion-transfer, and electron-transfer equilibria, could be determined also. These equilibria led to a great wealth of thermochemical data from this and many other laboratories, on the effect of gas-phase acidity and basicity, on the stability of carbocations and on the electron affinities of molecules. A brief account of these results and their significance is given in Sections 2.2–2.5. The data on ion-ligand bond energies are discussed in Section 2.6.

2. Some selected results from ion-molecule equilibria determinations

2.1. Formation of $H_3O^+(H_2O)_n$ ions in the D region of the ionosphere

Narcisi and Bailey [24] observed with rocket-borne mass spectrometers in 1965 that the ions H_3O^+ $H_3O^+(H_2O)$ and $H_3O^+(H_2O)_2$ are the dominant ions in the lower D region of the ionosphere. The presence of these ions was considered very surprising. The major source of ionization in this region is cosmic rays, which would lead to abundant production of N_2^+ and O_2^+ ions from the N_2 and O_2 (by far the major neutral constituents of this region). The nitrogen ions $N^+{}_2$ were known to rapidly convert to O_2^+ ions by the electron-transfer reaction: $N_2^+ + O_2 = N_2 + O_2^+$, however, it was known [25] that the reaction $O_2^+ + H_2O = O_2 + H_2O^+$ was endoergic and does not occur at normal thermal conditions. Therefore, the formation of H_3O^+ could not be assumed to occur via the well-known exoergic reaction: $H_2O^+ + H_2O = H_3O^+ + OH$.

The presence of the hydronium hydrates in the D region represented not just a scientific curiosity. Ion-electron recombination in the ionosphere is one of the processes that control the electron density, and the electron density determines the properties of the plasma that is responsible for the reflection of radio waves from the ionosphere. The hydronium hydrates were expected to lead to large ion-electron recombination coefficients and be responsible for the observed plasma density in the D region. Furthermore, it was rumored, at that time, that understanding and controlling the plasma density in the ionosphere had become a topic of military interest connected with the desired early detection of ballistic missiles!

In our experiments with the α-particle mass spectrometer [4,5] (see the preceding section), we had observed the formation of the series: H_3O^+, $H_3O^+(H_2O)$, $H_3O^+(H_2O)_3$ in air which contained traces of moisture and therefore we knew that these ions are indeed produced at conditions very similar to those in the D region. Having just developed the pulsed electron instrument [16], we felt that we were in a position to discover the mechanism that led to hydronium hydrates. The great advantage of the pulsed system was that it provided a complete picture of the evolution of all ion species from $t \approx 0$ to $t \approx 1000$ μs.

This is shown in Fig. 1 [17], which illustrates the evolution of ions observed in 2 Torr O_2 containing 4 mTorr of H_2O at 307K. The insert (b) shows the ionic intermediates that follow the formation of O_2^+ by the

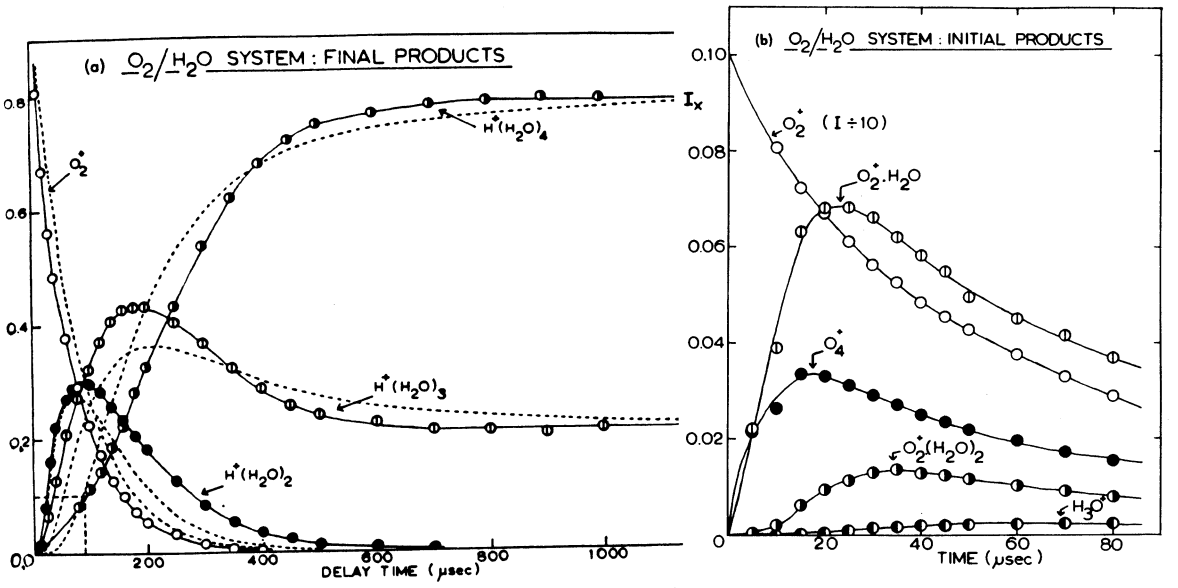

Fig. 1. Time dependence of major ions observed in O_2 at 3.5 Torr, containing traces (4 mTorr) of H_2O at 307K. Dashed lines represent calculated curves for reaction sequence. Enlarged cutout giving major ions in the first 80 μs provides a direct indication of reaction sequence: $O_2^+ \rightarrow O_4^+ \rightarrow O_2^+(H_2O) \rightarrow O_2^+(H_2O)_2 \rightarrow H_3O^+$, see text. Results obtained with PHPMS. This reaction sequence explains the observed presence of $H^+(H_2O)_n$ species in the D region of the ionosphere, see text. [Adapted from A. Good, D.A. Durden, P. Kebarle, J. Chem. Phys. 11 (1970) 222.]

short electron pulse. These intermediates indicate the reaction: $O_2^+ \rightarrow O_4^+ \rightarrow O_2^+(H_2O) \rightarrow O_2^+(H_2O)_2 \rightarrow H_3O^+$. On the other hand, Fig. 1(a) illustrates the development of the hydronium hydrates, the end products, which reach hydration equilibrium after some 600 μs.

The key reaction that leads to a switch from the $O_2^+(H_2O)_n$ hydrates to the hydronium hydrates was identified:

$$O_2^+(H_2O) + H_2O = [O_2^+(H_2O)_2]^* \rightarrow (H_3OOH)^+ + O_2 \quad (6a)$$

$$\rightarrow H_3O^+ + OH + O_2 \quad (6b)$$

$$\rightarrow O_2^+(H_2O)_2 \quad (6c)$$

where [17]

$$k_{6a} = 0.9\times10^{-9}\ \mathrm{cm^3 \cdot molecules^{-1} \cdot s^{-1}}$$

$$k_{6b} = 0.3\times10^{-9}\ \mathrm{cm_3 \cdot molecules^{-1} \cdot s^{-1}}$$

Reactions (6a,b) were exoergic because the excited complex $O_2^+(H_2O)_2$ allowed a combination of the endoergic charge transfer from O_2^+ to H_2O, with the exoergic formation of $H_3O^+ + OH$ from H_2O^+ and H_2O. In total, the rate constants for fourteen reactions involved in the mechanism, as well as equilibrium constants for the hydronium ion hydration reactions, were obtained.

Independently and close to simultaneously, Fehsenfeld and Ferguson [26] proposed a close-to-identical mechanism based on measurements with the flowing afterglow apparatus. However, in those early days, the rate data and directly observed reaction system obtained with the pulsed instrument [17] were more complete.

On the basis of the publication [17], my coworkers David Durden, Tony Good and I enjoyed, for a few years, the attention and hospitality of the scientific community working on the ionosphere. It was gratifying to be suddenly accepted in a totally new area and to be able to contribute to the discussions.

2.2. Proton transfer equilibria: gas-phase basicities and acidities

Although we had realized the fundamental importance of the ion-ligand and ion-solvent molecule equilibria data, we were somewhat slow to expand the measurements to other types of equilibria, particularly, the important class of proton-transfer equilibria. At the time there were alternate methods that provided proton affinities [27], such as appearance potentials. For example, the appearance potential of the H_3O^+ ion from the electron ionization of ethanol, could be combined with available thermochemical data to yield the proton affinity of H_2O [28]. Although the accuracy of such determinations was not well established, the method seemed legitimate.

I was prompted to start proton-transfer equilibria determinations by one of my former doctoral students, Ismet Dzidic, who at that time was doing postdoctoral work at Baylor College of Medicine, in the group directed by Margorie and Evan Horning. This group was then developing atmospheric pressure ionization (API) as an analytical method. Dzidic, in one of his phone calls in 1970, urged me to start proton-transfer equilibria determinations, because abundant and accurate proton affinities would be a very useful background for understanding the mass spectrometric observations under API conditions. We initiated the measurements at that time, selecting nitrogen bases such as: NH_3, CH_3NH_2, $(CH_3)_2NH$, pyridine and $(CH_3)_3N$. It turned out that these bases spanned a rather wide proton affinity range of some 24 kcal/mol [29,31].

The proton transfer equilibrium measurements

$$AH^+ + B = A + BH^+ \tag{7a}$$

$$\Delta G^\circ_{PT} = RT \ln K_{PT} \qquad K_{PT} = \frac{[BH^+][A]}{[AH^+][B]} \tag{7b}$$

where $K_{PT} = [BH^+][A]/[AH^+][B]$, lead to ΔG°_{PT}, which corresponds to the gas-phase basicity difference, whereas ΔH°_{PT} corresponds to the proton affinity difference:

$$\Delta G^\circ_{PT} = \Delta G^\circ_B(A) - \Delta G^\circ_B(B) \tag{7c}$$

Successive ΔG°_{PT} involving a series of bases are combined in a ladder (scale) of relative values. For examples of such ladders, see Figures 4 and 5. To obtain the absolute gas-phase basicity or proton affinity, one needs to calibrate the ladder to one absolute value obtained by some other method.

To cover a range of 24 kcal/mol, while using only a few bases, required the determination of some rather large ΔG°_{PT} values such as was the case for NH_3 and CH_3NH_2 for which the $\Delta G^\circ_{PT} \approx 10.8$ kcal/mol, corresponding to a $K_{PT} \approx 9 \times 10^3$. This was well within the range of the PHPMS with which a neutral offset ratio as high as $[A]/[B] = 10^3$ and an ion offset ratio as high as $BH^+/AH^+ = 10^3$ also could be measured accurately. The temperature dependence of K_{PT} could be determined allowing evaluation of ΔG°_{PT} at different temperatures, and the corresponding ΔH°_{PT} values.

It took over a year to complete this first proton transfer equilibrium study [29,30]. It was only after having submitted the results for publication that we learned that proton transfer equilibria had been determined recently [31] with a pulsed electron trapped ion cell, ion cyclotron resonance (ICR) instrument developed by Bob McIver [32, see also 33,34].

Even though we felt that our PHPMS method was superior for the proton-transfer equilibria determinations, particularly because the temperature was well defined, we now had powerful competition from ICR practitioners, which included several outstanding chemists. In the long run, the competition proved beneficial, not only to the development of the thermochemistry based on equilibria and the associated applications of that thermochemistry, but also to our own work, since we could learn much from our competitors.

Within a relatively short time, a continuous proton-affinity scale was developed (see Fig. 2). The scale started with compounds of very low basicity, such as the σ-electron base H_2, increasing over σ-electron bases like CH_4 and C_2H_6 [35,36], then further to π-electron bases like the olefins and benzene, then to weak oxygen bases like H_2O and stronger oxygen bases such as alcohols, ethers, ketones, up to the weak nitrogen base NH_3 [37–39], then progressing through a great variety of organic nitrogen bases [29–31,34,

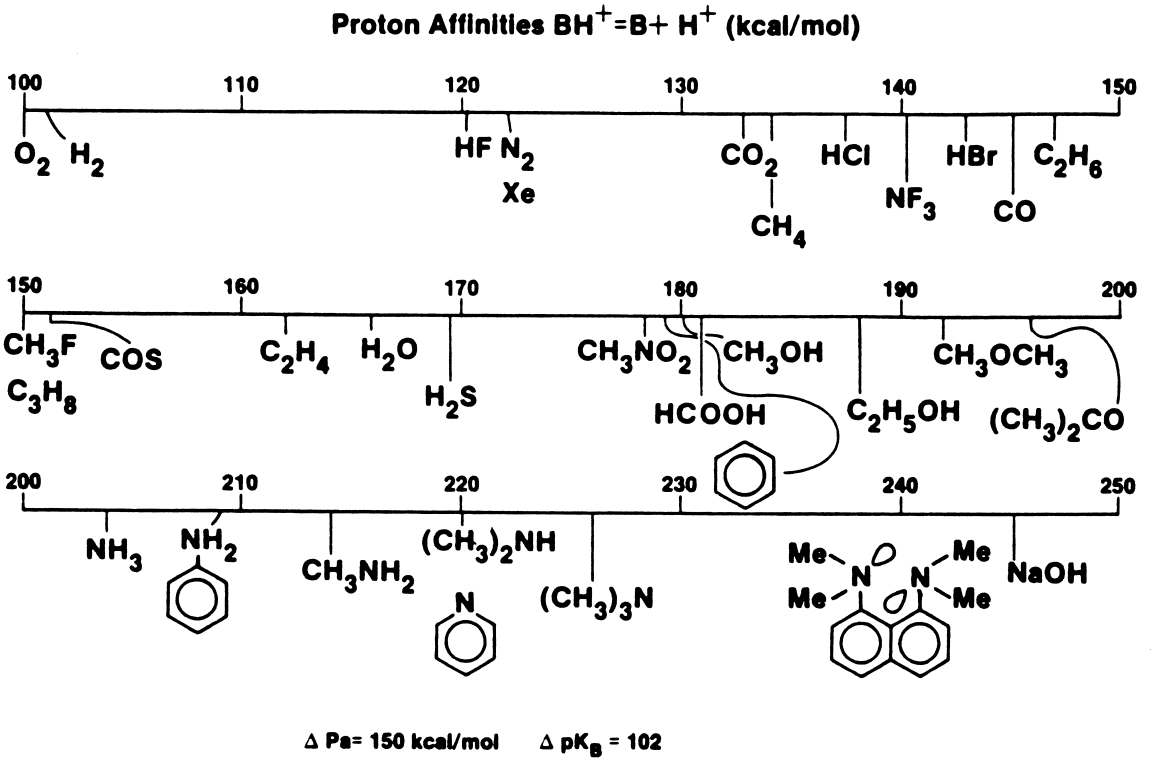

Fig. 2. Schematic view of the proton affinity scale of bases B, which extends over some 150 kcal/mol, starting with weak (σ-electron bases) like H_2 and ending with highly basic organic compounds like the proton sponge, 1,8-*bis*(dimethylamino)naphthaline, where the proton is not only dicoordinated by the two nitrogen bases $N(CH_3)_2$, but where the protonation also releases steric strain caused by repulsion of the two lone pair of electrons of the two groups, present in the neutral proton sponge.

40–42], finally culminating with ultra-strong bases like 1,8-*bis*(dimethylamino)naphthalene (proton sponge) [43], where the proton is stabilized by dicoordination to the two adjacent dimethylamino groups. Steric strain due to repulsion between the two lone pair orbitals of the dimethylamino groups present in the neutral base (see Fig. 2) is released on protonation, and this effect leads to an additional increase of proton affinity.

The calibration to absolute values of the relative proton affinity scale in order to obtain an absolute affinity scale proved to be more difficult than had been expected. The main problem was that absolute values available from appearance potential measurements and associated supporting thermochemical data proved unreliable, that is, absolute markers at different positions in the scale led to different absolute values for the scale. Ultimately, it was mainly a combination of experimental measurements and high-level ab initio calculations for the protonated small bases (CO, C_2H_4) which led to the presently accepted absolute scale [44]. For a detailed account see Szuleiko and McMahon [44]. These authors obtained the scale on the basis of measurements of the temperature dependence with a PHPMS, of a large number of key proton transfer equilibria and a detailed study of absolute values available in the literature.

Gas-phase acidities of neutral acids AH, such as, for example, carboxylic acids like formic acid and acetic acid or inorganic acids like HCl or HNO_3, can be determined from proton transfer equilibria.

$$AH + B^- = A^- + BH \quad (8)$$

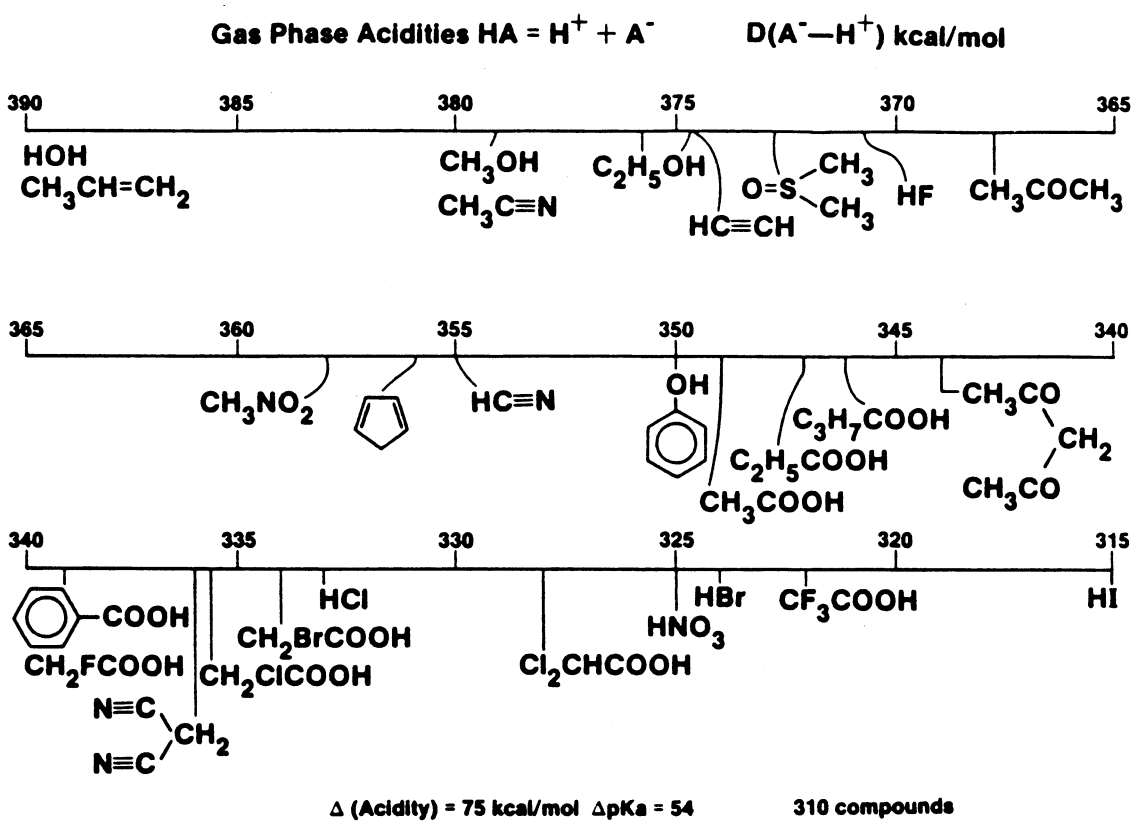

Fig. 3. Schematic view of the gas-phase acidity scale of acids AH, which extends from relatively weak oxygen acids like H_2O and carbon acids like propylene and extends to relatively strong acids like nitric acids HNO_3. Note some obvious reversals relative to acidity in aqueous solution, such as CF_3CO_2H being a stronger acid than HNO_3, in the gas phase.

Similarly to the proton transfer equilibria involving neutral bases, relative acidity scales are obtained from determinations of the equilibrium constants K_8 leading to ΔG°_8 and ΔH°_8.

The relative acidity scale can then be calibrated to provide the absolute acidity corresponding to

$$AH = A^- + H^+ \qquad \Delta G^\circ_9, \Delta H^\circ_9 \tag{9}$$

by using thermochemical data available in the literature. This ΔH°_9 can be obtained from

$$\Delta H^9 = \Delta H^\circ_9(AH) = D(A{-}H) - EA(A) + IE(H) \tag{10}$$

where D(A–H) is the bond dissociation enthalpy, EA(A) is the electron affinity of A and IE(H) is the ionization energy of the hydrogen atom. For the diatomic hydrogen halides HX = HF, HCl, HBr, HI, good values for the above quantities were available in the literature and therefore, the calibration of scales obtained from proton transfer equilibria, which included HX compounds, was relatively straightforward [45–50].

The gas-phase acidity scale involving stronger acids AH, such as phenols, the carboxylic acids, the hydrogen halides HX, HNO_3, was obtained by PHPMS determinations [45-50], while the weakly acidic alcohols and carbon acids were obtained by Miller, Bartmess Scott and McIver [51–53], using ICR. A schematic representation of the acidity scale is shown in Fig. 3. The strongest acid shown on this scale is HI. HI is stronger than the other HX acids primarily because of the weak H–I bond. More

recently, the scale was extended to include stronger acids, such as HPO_3, H_2SO_4, $HFSO_3$ and CF_3SO_3H [55].

On the basis of proton transfer equilibria measurements, the basicity and acidity of many thousands of neutral bases B and acids AH have been determined. These data have been collected in the NIST Database (http://webbook.nist.gov/chemistry/, see also; for bases, Hunter and Lias [56] and for acids, Bartmess [57].

The major impact of the above data occurred initially in organic chemistry. The basicity order of many organic bases in aqueous solution was often very different from that observed in the gas phase and the same was true for organic acids. For example, aniline and pyridine were found to be stronger gas-phase bases than NH_3 but in solution they were known to be weaker bases. Obviously this meant that the effect of the solvent was very important in determining the relative strength of the bases and acids. However in many cases, the basicity (or acidity) orders in solution had been rationalized on the basis of the electronic structure of the given base (or acid), namely, properties intrinsic to the molecules that should have shown up also in the gas phase.

Examples are the basicities of alkyl amines. The ΔG°_{PT} values for proton transfer from NH_4^+ to the amines in water and the gas phase are given below.

	NH_3	$MeNH_2$	Me_2NH	Me_3N	
$-\Delta G_{PT}$ (w)	0	1.9	2.1	0.8	(kcal/mol)
$-\Delta_{PT}$ (g)	0	9.5	15.8	20.4	(kcal/mol)

The change in water is much smaller; furthermore in water the basicity increases slowly up to Me_2NH and then goes down for Me_3N, while a continuous increase with Me substitution is observed in the gas phase. The reversal of the effect of Me in water between Me_2N and Me_3N, known as the amine anomaly had been much discussed in the literature on organic chemistry. Some considered that this is due to an intrinsic property of the molecules, whereas others proposed solvation effects (namely, the decreasing number of protic hydrogens that can hydrogen bond to water in the protonated species in the order NH_4^+ to Me_3NH^+) to explain the amine anomaly. The gas-phase data eliminated the possibility that this is an intrinsic effect, thus confirming that solvation differences were the cause. For a detailed analysis see Arnett et al. [58].

The stabilization of the protonated bases in the gas phase by the alkyl groups is due mainly to the polarizability of these groups, however some σ-electron donation to the nitrogen is also involved. The decrease of solvation of the alkylated protonated bases is due to two factors: First, the bulky organic groups displace solvent. Second, because of the stabilization by the alkyl groups, the protic hydrogens on the nitrogen are less acidic and form weaker hydrogen bonds to the surrounding water molecules. Therefore, most organic nitrogen bases, including the basic peptide residues like arginine, histidine and lysine, are very much stronger bases than NH_3, in the gas phase. This circumstance is of importance in the important analytical methods, MALDI and ESI, because it leads to facile formation of the protonated analyte ions in the transfer from solution to the gas phase.

2.3. Hydride ion and chloride ion transfer equilibria—stabilities of carbocations

Hydride or chloride transfer equilibria

$$R_o^+ + RH = R_oH + R^+ \quad (11)$$

$$R_o^+ + RCl = R_oCl + R^+ \quad (12)$$

have been used to obtain values for the relative stabilities of carbocations R^+ and, when associated thermochemical data are available, also the enthalpies of formation, $\Delta H_f^\circ(R_+)$. Hydride ion affinity scales were first obtained by Mautner and Field [59–62], based on equilibria determined with a high-pressure mass spectrometer. Later, PHPMS determinations of hydride and chloride transfer equilibria were determined in this laboratory [63]. A ladder of ΔG°_{11} from chloride transfer equilibria determinations [63] is shown in Fig. 4. The carbocations R^+ are substituted

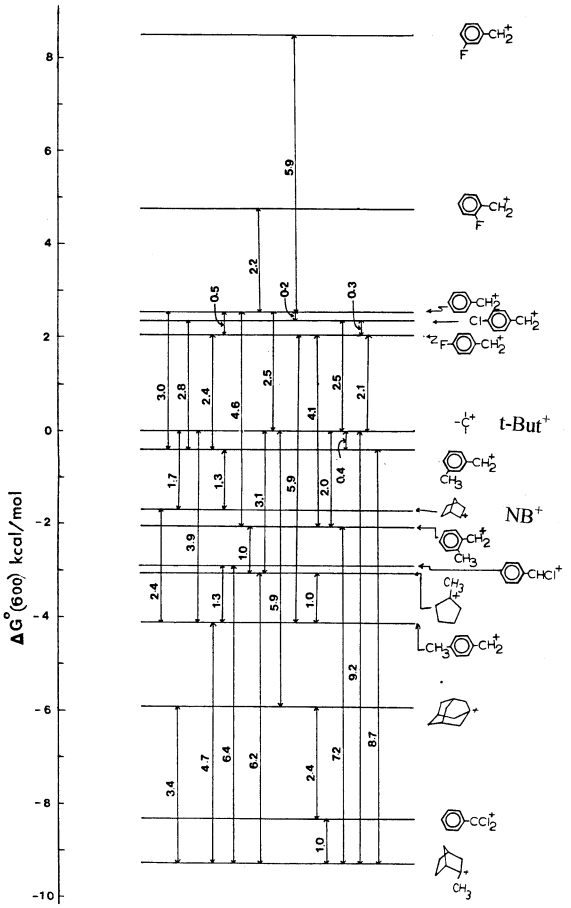

Fig. 4. Ladder of ΔG° values for chloride transfer equilibria: $RCl + R_o^+ = R^+ + R_oCl$ determined in the gas phase. The carbocations R^+ are shown in the figure. This scale demonstrates that the 2-norbornyl cation NB^+, whose classical structure is shown in the scale, is more stable than the tertiary butyl cation *t*-But^+. This high stability is not compatible with the classical secondary alkyl cation structure but with the nonclassical σ-electron-bridged Structure I. [Adapted from R.B. Sharma, D.K. Sharma, K. Hiraoka, P. Kebarle, J. Am. Chem. Soc. 107 (1985) 3747.]

benzyl cations, some tertiary alkyl carbonium ions like tert-butyl and the secondary cation norbornyl.

Carbocations play a very significant role in organic synthesis and were also very much involved in the development of physical organic chemistry. The work [63] was aimed to a large measure as a contribution towards resolving one famous controversy in physical organic chemistry, namely the so-called "classical or nonclassical structure of the norbornyl cation". For a

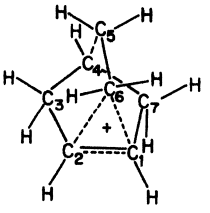

Structure 1.

compact modern summary see Ref. 63. The proponents of the nonclassical view held that the norbornyl cation is unusually stable because it is stabilized by σ-bridging as shown in the nonclassical Structure I.

The classical structure, NB^+, in which the cation is a secondary alkyl ion is shown in the affinity ladder (Fig. 4). The order of carbocation stabilities, which increases from top to the bottom in Fig. 4, clearly shows that the norbornyl cation is more stable than tertiary butyl and much more stable than could be expected for a classical secondary alkyl carbocation. The results from these [63] and other [68,69] gas-phase ion equilibria determinations, as well as ab initio theoretical calculations showing that Structure I is the most stable structure [64–67] were decisive in resolving the controversy in favor of the nonclassical Structure I. It should be noted that previous efforts to resolve it by experimental work in the condensed phase had involved a vast research effort stretching over close to three decades [64–67].

2.4. Methyl cation transfer equilibria

Methyl cation transfer equilibria

$$MeB_0^+ + B = MeB^+ + B_0 \qquad (13)$$

involve the Me^+ cation, which has a low-energy empty orbital and behaves as a Lewis acid, and Lewis bases B, which are the electron donors. Methyl affinity scales can be established on the basis of determination of equilibria (see Eq. 13), and methyl cation affinities (MCA) can be

$$MeB^+ = Me^+ + B \quad \Delta H_{14}^+ = MCA\ (B) \qquad (14)$$

determined from the scales by calibrating to the absolute value for one base B. MCA studies in the gas

phase were initiated by Beauchamp [70]. However, abundant data on MCA became available only through the Me^+ transfer equilibria [71].

MCA data have application to both processes in the gas phase and in solution. Many molecules observed in interstellar space correspond to MeB^+ and it is assumed that they are formed by the reverse of Eq. (14) in interstellar clouds and dust [72,73] from molecules B = Ne, H_2, O_2, CO, CO_2, and so on. Important processes in solution include:

1. The methylation and alkylation in organic synthesis undertaken with the use of diazonium ions MeN_2^+ and RN_2^+ or halonium ions $MeXR^+$ [74].
2. Alkylating agents are believed to achieve carcinogenic activity by conversion to highly reactive diazonium cations, $MeN_2{}^+$ or $RN_2{}^+$, which then alkylate the nucleophilic basic sites in DNA [75].

Recent work by Gluhorster et al. [76] provides an update of the MCA thermochemistry.

2.5. Electron affinities of molecules from electron-transfer equilibria

The electron affinities of molecules are of interest not only in areas where gas-phase ions are encountered (e.g. negative ion analytical mass spectrometry [77], the ionosphere [78], gaseous electronics [79], electron capture detector gas chromatography [80,81]), but also in the much wider field of condensed phase chemistry. Charge transfer complexes and their role in organic and biological processes represent a vast area for which knowledge of the electron affinities is of prime importance [82,83]. Reductions through single electron transfer from alkali metals to unsaturated organic compounds (e.g. Bouvault-Blank, Birch) have been of importance in organic synthetic chemistry for many years.

Relative electron affinities of molecules A, B can be obtained from electron-transfer equilibria in the gas phase

$$A^- + B = A + B^- \quad \Delta H^\circ_{14} = EA(A) - EA(B) \tag{15}$$

$$A^- = A + e \quad \Delta H^\circ_{16} = EA(A) \tag{16}$$

Absolute electron affinities of high accuracy can be obtained by photodetachment techniques [84,85], however the molecules involved should be relatively small, preferably diatomic or triatomic. Therefore, prior to the introduction of electron-transfer equilibria few reliable electron affinities for larger molecules were available. However, the electron affinities from photodetachment such as that for SO_2, provided excellent anchors for the calibration of electron affinities obtained from electron-transfer equilibria.

Fukuda and McIver, using a pulsed, trapped-ion ICR mass spectrometer [86,87], were the first to determine electron-transfer equilibria. However they encountered difficulties that led to an erroneous calibration of their scale, which contained some 15 compounds. Later, work from this laboratory based on PHPMS, led to a correct calibration that agreed with photodetachment values and extended the scale to some 160 compounds [88–90].

Typically, organic compounds with positive electron affinities possess conjugated double bonds, which leads to relatively low-lying LUMOs, which accept the extra electron. For smaller conjugated systems, the LUMO may not be low enough, and then the presence of an electron-withdrawing substituent (F, Cl, CHO, CN, NO_2) is required to lower the LUMO energy and lead to a stable radical anion. Thus, benzene does not lead to a stable radical anion but nitrobenzene does.

A ladder obtained from electron-transfer equilibria and the electron affinities resulting from calibration of the ladder is shown in Fig. 5. Anions of compounds with electron affinities lower than ~10 kcal/mol are unstable to thermal electron detachment at room temperature and electron-transfer equilibria need to be determined at lower temperatures.

2.6. Ion-ligand L and solvent S molecule equilibria

The determination of ion-ligand or ion-solvent molecule equilibria was considered briefly in Section 1. Since the initiation of these measurements [3–17], a vast number of determinations have been performed by this group and other investigators. Notable have been the contributions by Castleman and coworkers

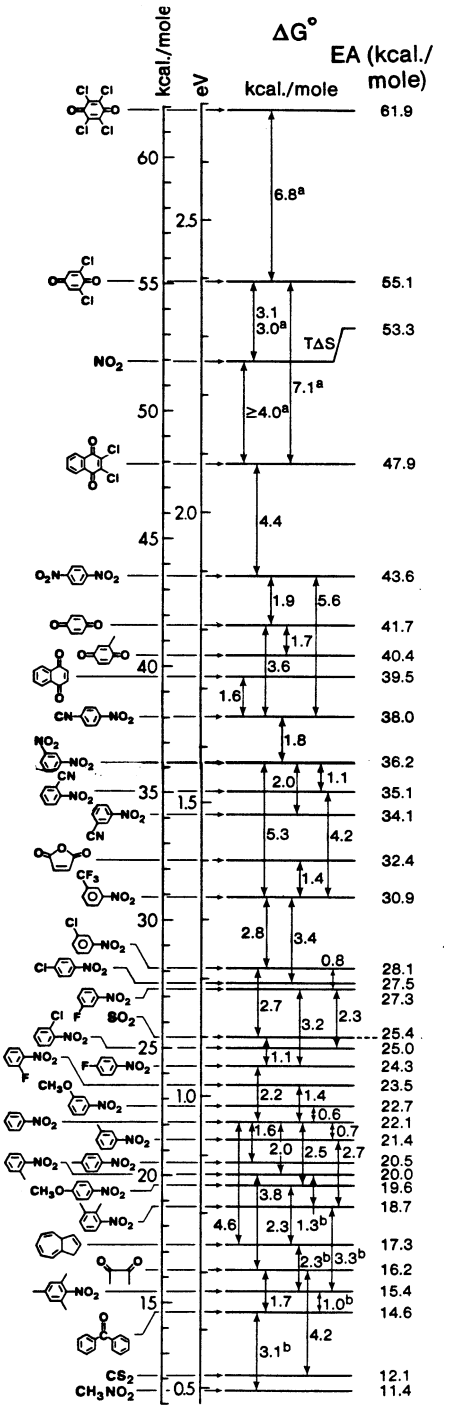

Fig. 5. Electron affinity scale of molecules, which become radical anions on accepting an electron. [Adapted from E.P. Grimsrud, G. Caldwell, S. Chowdhury, P. Kebarle, J. Am. Chem. Soc. 107 (1985) 4627.]

and Meot-Ner (Mautner) and coworkers both of which used HPMS instruments. Early work was summarized by Kebarle [91]. Keesee and Castleman [92] have provided a more recent review, while the most recent thermochemical data compilation is due to Meot-Ner and Lias [93].

We will consider here only a few results and their use to illustrate the area. Results for multiply charged ions, obtained by electrospray, are considered in the next section. The early utilization of the gas-phase data was focused on creating a bridge between ion-molecule processes in the gas phase and in solution. For example, the enthalpy changes $\Delta H^\circ_{n-1,n}$ for the hydration of the alkali ions M^+ obtained from gas-phase equilibria [13]

$$M^+(H_2O)_{n-1} + H_2O = M^+(H_2O)_n$$

are shown in Fig. 6. The $\Delta H^\circ_{1,0}$ increase in the order Cs^+, Rb^+, K^+, Na^+, Li^+ as expected due to the decreasing size of the ions in that order. However already at $\Delta H^\circ_{5,4}$ and $\Delta H^\circ_{6,5}$ the values for all the above ions have become quite similar. This suggests that the differences in the enthalpy of solvation of these ions in aqueous solution are reflected principally in the differences of the $\Delta H^\circ_{0,n}$, where n is as small as 6 or 7. That this is the case is indicated by the data in Fig. 7, which show the difference $\Delta H^\circ_{0,n}$ $(Cs^+) - \Delta H^\circ_{0,n}$ (M^+), where $M^+ = Rb^+$ to Li^+. The extrapolated values at high n are very close to the difference for the corresponding hydration enthalpy differences: ΔH°_h $(Cs^+) - \Delta H^\circ_h$ (M^+), obtained from data in the literature.

The total hydration energies ΔH°_h (M^+) correspond to the enthalpy change

$$M^+(g) \xrightarrow{H_2O(l)} M^+(aq) \qquad \Delta H^\circ_h(M^+)$$

for the transfer of the ion from the dilute gas phase to aqueous solution. Such values can be obtained on the basis of thermodynamic cycles and experimental measurements involving M^+X^- salts [94]. The results in Fig. 7 illustrate that the initial interactions are domi-

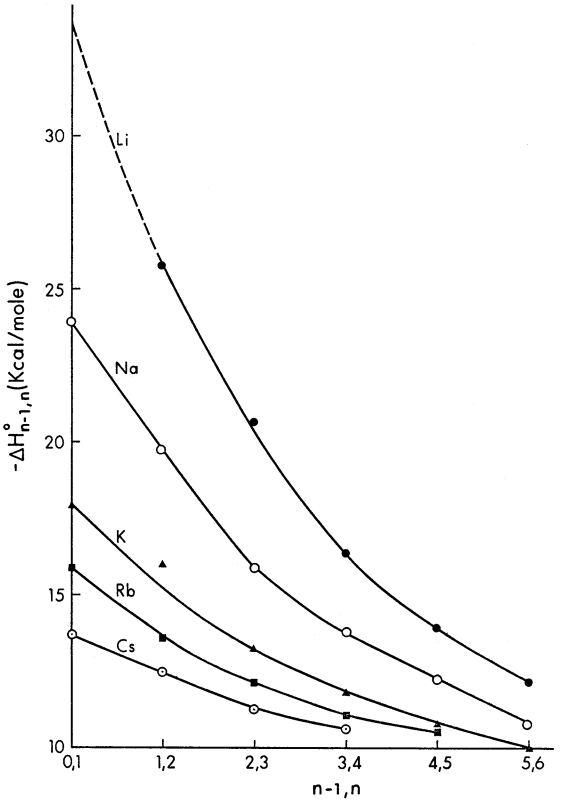

Fig. 6. Enthalpy changes, $-\Delta H^{\circ}_{n-1,n}$ for hydration reactions: $M^+(H_2O)_{n-1} + H_2O = M^+(H_2O)_n$, where M^+ are the alkali ions: Li^+, Na^+, K^+, Rb^+, Cs^+. Note, that at high n, the $\Delta H^{\circ}_{n-1,n}$ become close to being the same for all M^+. This means that the hydration enthalpies in aqueous solution $\Delta H^{\circ}_n(M^+)$, for the different M^+ are essentially determined by the sum of the initial interactions $\Delta H^{\circ}_{0,n}$, where n can be as small as 8 or 9. [Adapted fromI. Dzidic, P. Kebarle, J. Phys. Chem. 74 (1970) 1466.]

nant and can be used to probe trends involving ions in solution. This approach is very attractive because the interactions of one ion with one or more solvent molecules can be easily understood. On the other hand the interaction of an ion with the totality of the solvent appears a daunting task. The ion solvent molecule approach is illustrated by the following example.

Dipolar aprotic solvents, that is, solvents with large dipoles but no protic hydrogens such as acetonitrile (MeCN) or dimethylsulfoxide (Me_2SO), have special utility in synthetic organic reactions involving negative ions, such as S_N2 reactions. Much faster rates are observed with these solvents when compared to rates in protic solvents like water and ethanol. Although the utility of using polar diprotic solvents was appreciated, the reason why these solvents were superior was not well understood. Measurements of the $\Delta G^{\circ}_{0,n}(X^-)$ and $\Delta H^{\circ}_{0,n}(X^-)$ for ions $X^- = Cl^-, Br^-, I^-$ with H_2O and Me_2SO molecules in the gas phase showed that Me_2SO solvation exothermicity decreases, with increase of ion radius, much more slowly than is the case with water (or methanol) [95]. This was shown as being due to the dipole of Me_2SO which is located largely on the SO group. The dipole is relatively far away from the negative X^-, due to the steric hindrance by the two methyl groups [95], and this makes the interaction with X^- less sensitive to increases of the X^- radius in the series Cl^-, Br^-, I^-. The transition state in S_N2 reactions such as $Cl^- + CH_3Br = ClCH_3 + Br^-$, is a negative ion which is larger than the initial Cl^- ion. The energy of the transition state is higher than that of the reactants only because of the poorer solvation of the bigger transition state ion relative to Cl^- [96,97]. The beneficial effect of Me_2SO and other dipolar aprotic solvents is therefore a consequence of the relative insensitivity of these solvent molecules to the increase of ion radius [95]. Dipolar aprotic solvents, while solvating negative ions weakly, solvate positive ions strongly, because the large dipoles of these solvent molecules can approach closely the positive ions. Therefore ion pairs M^+X^- as a whole are sufficiently soluble in such solvents [95]. This solubility allows the use of these solvents to advantage for synthetic work involving reactions of negative ions.

The very first experimental results on sequential hydration of the ions like H_3O^+, NH^+_4 and the alkali ions and halide negative ions [7,8,13,14], stimulated many theoretical ab initio calculations for the same systems [98-108]. The experimental results were particularly useful in indicating that only very large basis sets would lead to agreement between theory and experiment. The theoretical work was soon extended toward development of ion-molecule pair potential functions which could be used for modeling of the interactions of an ion

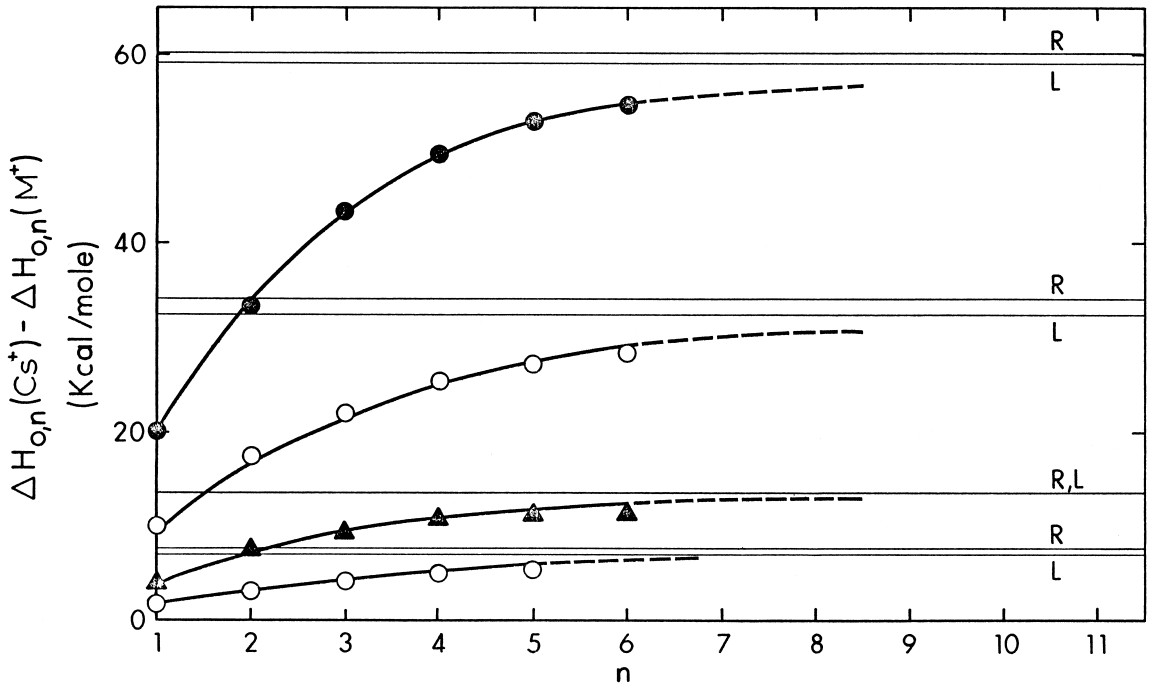

Fig. 7. Plots of $\Delta H^{\circ}_{0,n}(M^+)$, see Figure 6, plotted as differences: $\Delta H^{\circ}_{0,n}(Cs^+) - \Delta H^{\circ}_{0,n}(M^+)$. ●, $M^+ = Li^+$; O, $M^+ = Na^+$; ▲, $M^+ = K^+$; bottom plot $M^+ = Rb^+$. Horizontal lines represent values of $\Delta H^{\circ}_h(Cs^+) - \Delta H^{\circ}_h(M^+)$ for the hydration energies in liquid water, where the individual ΔH°_h values are from two literature sources, Latimer, Pitzer, Slauski = L or Randles = R. This plot proves the proposition in the caption of Fig. 6. [Adapted from I. Dzidic, P. Kebarle, J. Phys. Chem. 74 (1970) 1466.]

with a group of solvent molecules by Monte Carlo or Molecular Dynamics methods [103–108].

2.7. Ion-ligand interactions involving multiply charged ions produced by electrospray. modeling of the reactive centers of enzymes

The results described in the previous sections involved singly charged ions, yet doubly and triply charged ions such as Mg^{2+}, Ca^{2+}, Zn^{2+}, Cu^{2+}, Fe^{2+}, Fe^{3+} are of paramount importance in chemistry and particularly biochemistry. Different methods need to be used to be able to study ion-ligand systems involving these ions. In the previous studies, the naked ion M^+ was produced and the ligands were added as a vapor. This method often does not work with multiply charged ions. The forward clustering reactions for many of these ions are displaced by faster charge separation reactions, which lead to two singly charged ions [109].,

The most convenient method to produce multiply charged ion-ligand complexes is electrospray developed by J.B. Fenn and colleagues [110,111]. Electrospray is a method by which ions present in solution can be transferred to the gas phase, and an extraordinary variety of ion-ligand complexes involving ions such as Li^+, Na^+, K^+, Rb^+, Cs^+, Be^{2+}, Mg^{2+}, Ca^{2+}, Se^{2+}, Cr^{2+}, Zn^{2+}, Mn^{2+}, Fe^{2+}, Co^{2+}, Co^{3+}, Ni^{2+}, Cu^+, Cu^{2+}, Ag^+, and so on can be produced by electrospray [112,113].

An ion source in which ions produced by electrospray can be equilibrated with ligand vapor and the ion-ligand equilibria determined with a mass spectrometer was developed recently [114]. Here, we describe only one of the many applications of such equilibria determinations.

The ligand compositions of the reactive centers of

three Zn metalloenzymes are shown below. It is notable that the histidine residue is used very often in the above complexes and this ligand is present often in reactive centers of other metalloenzymes. We became interested in understanding why histidine is used so often.

A study of the binding energies in Cu^+L_2 complexes based on ligand transfer equilibria measurements [115] showed that of all amino acids, histidine, whose functional group corresponds to imidazole, leads to the strongest bonding with Cu^+. Because Cu^+ is isoelectronic with Zn^{2+}, histidine is expected to be the strongest binding of all peptide residues also for Zn^{2+}. This indicates that the strongly bonding histidine fulfills one essential function, which is to provide stability for the Zn^{2+} ion within the enzymes relative to the aqueous environment outside the enzyme.

For carbonic anhydrase, this supposition could be proved [116], on the basis of the binding energies [116] of the ligands in the reactive center, $Zn(Im)_3(H_2O)^{2+}$. The sum of the binding energies was found to be equal to 340 kcal/mol [see Table 2 in Ref.116]; that is, the complex in the gas phase had a stabilization energy of −340 kcal/mol. The total hydration energy of Zn^{2+} is ΔG_h° $(Zn^{2+}) = -470$ kcal/mol [94]. It could be shown that additional stabilization of the $Zn(Im)_3(H_2O)^{2+}$ complex due to H bonding and solvation interactions with the enzyme environment lead to a total stabilization energy larger than the hydration energy of Zn^{2+} and thus to a just-sufficient stability of Zn^{2+} in the enzyme [116].

The initial ion-ligand bonding interactions, when doubly charged ions like Zn^{2+} and strongly bonding ligands like imidazole are present, are very strong, and these bond energies could not be obtained by ion-ligand equilibria determinations. These data had to be obtained by theoretical calculations [116]. However as the number of ligands increases, the sequential bond energies decrease due to ligand–ligand repulsions and charge transfer from the ligands, so that the bond energies for later ligands can be obtained by ion equilibria.

Another question needs also to be answered: Why was the specific ligand composition of the reactive centers for the different Zn^{2+} enzymes (see Structures 2) chosen in the evolutionary process? An answer to this question could be provided also [116]. The choice of the first three ligands has a strong effect on the bonding of the fourth ligand which is H_2O. Strongly electron-donating ligands weaken the bonding of the H_2O ligand. This is illustrated by the data provided in Table 1. The H_2O ligand is the only ligand that is involved in the actual reaction that is catalyzed by the enzyme, and the bond energy of the H_2O ligand must be exactly tuned to the requirement of this catalysis. It could be shown [116] that for the reaction catalyzed by carbonic anhydrase, the required bond energy of

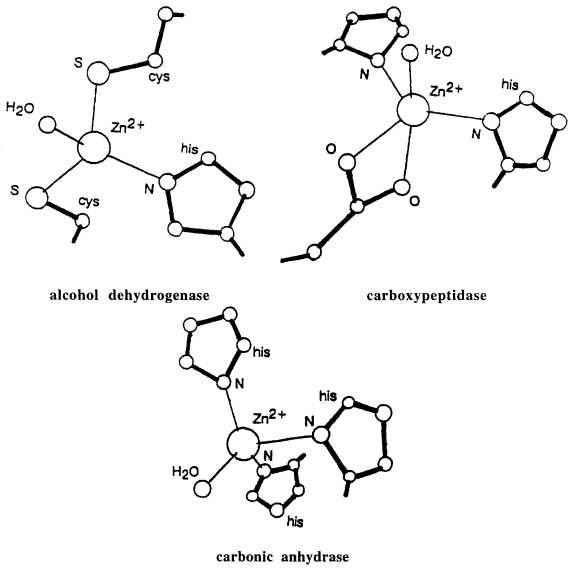

Structures 2.

Table 1
How choice of first three ligands determines the bond-free energy of the fourth (reactive) ligand[a]

Reaction	ΔG° kcal/mol
$Zn(H_2O)_3(H_2O)^{2+} = Zn(H_2O)_3^{2+} + H_2O$	34.3 (theor.)[b]
$Zn(NH_3)_3(H_2O)^{2+} = Zn(NH_3)_3^{2+} + H_2O$	22.5 (theor.)[b]
$Zn(Im)_3(H_2O)^{2+} = Zn(Im)_3^{2+} + H_2O$	12.0 (theor.)[b]
	14.0 (exp.)[c]
$Zn(Im)_2CH_3CO_2(H_2O)^+$	5.0 (exp.)[c]
$= Zn(IM)_3CH_3CO_2)^+ + H_2O$	

[a]Selected values [from Table 3 in Ref. 79].

[b]Theoretical calculations at the B3LYP/6-311++G(d,p) level [79].

[c]From ion-ligand equilibria, involving hydration of $Zn(Im)_e^{2+}$ and $Zn(Im)_2CH_3CO_2)^+$ complex produced by electrospray [79].

the H_2O ligand was close to ~13 kcal/mol, that is, equal to the bond energy provided by the presence of three imidazole (his) ligands in carbonic anhydrase.

Carbonic anhydrase [116] is amenable to the application of gas-phase energetics. The major difficulty was the inclusion of the effect of the environment surrounding the reaction complex (i.e. the rest of the enzyme and the aqueous solution outside) on the values of the reaction energies obtained in the gas phase. The results obtained were therefore only of a semiquantitative character. Nevertheless, such approaches can provide valuable thermochemical insights, which are very much needed in biochemistry.

2.8. Application of gas-phase ion equilibria data to modern analytical mass spectrometry

The applications described in the previous sections dealt mostly with relationships between the energetics in the gas phase and those in solution. The gas-phase data, such as gas-phase basicities, acidities and ion-molecule bond energies have, of course, also direct applications to analytical mass spectrometry such as electrospray mass spectrometry (ESMS). With this method, preexisting ions in solution are transferred to the gas phase. Therefore, the thermochemical properties of the ions in solution and in the gas phase are of importance.

This is particularly the case when one tries to understand why certain analyte ions are observed in abundance, in the gas phase, whereas others are not. Thus one cannot under ordinary conditions, observe deprotonated negative ions from sugars, because the gas-phase acidities of these hydroxy compounds are very low. On the other hand, one readily observes the Na^+ adducts and this is to be expected because these ions are known to bond strongly in the gas phase to hydroxy groups containing analytes.

The observed state of protonation of multiply protonated peptides and proteins can be understood on the basis of the high proton affinities of the basic peptide residues such as His, Arg, Lys, Trp [117]. In the gas phase, stabilization of the proton can occur intramolecularly [118,119], as expected from early work on the cyclization of diamines [30], or by strong hydrogen bonding to solvent molecules. All these factors need to be considered in attempts to predict the observed state of protonation [120].

The above examples are a small sampling of applications of gas-phase thermochemistry data in ESMS. It is clear that such data will continue to provide a needed background for the development of interpretations of the observed mass spectra and the mechanisms of ion formation in ESMS.

References

[1] L.L. Kiefer, C.A. Fierke, Biochemistry 33 (1994) 15233.
[2] D.R. Bundle, B.W. Sigurskjold, Meth. Enzymol. 242 (1994) 288.
[3] P. Kebarle, E. Godbole, J. Chem. Phys. 36 (1962) 302.
[4] P. Kebarle, E.W. Godbole, J. Chem. Phys. 39 (1963) 1131.
[5] A.M. Hogg, P. Kebarle, J. Chem. Phys. 43 (1965) 449.
[6] P. Kebarle, A.M. Hogg, J. Chem. Phys. 42 (1965) 798.
[7] A.M. Hogg, R.N. Haynes, P. Kebarle, J. Am. Chem. Soc. 88 (1966) 28.
[8] P. Kebarle, S.K. Searles, A. Zolla, J. Scarborough, M. Arshadi, J. Am. Chem. Soc. 89 (1967) 6393.
[9] P. Kebarle, R.N. Haynes, J.G. Collins, J. Am. Chem. Soc. 89 (1967) 5753.
[10] S.K. Searles, P. Kebarle, J. Phys. Chem. 72 (1968) 742.
[11] P. Kebarle, M. Arshadi, J. Scarborough, J. Chem. Phys. 49 (1968) 817.
[12] P. Kebarle, M. Arshadi, J. Scarborough, J. Chem. Phys. 50 (1969) 1049.
[13] I. Dzidic, P. Kebarle, J. Phys. Chem. 74 (1970) 1466.
[14] M. Arshadi, R. Yamdagni, P. Kebarle, J. Phys. Chem. 74 (1970) 1475.
[15] M. Arshadi, P. Kebarle, J. Phys. Chem. 74 (1970) 1483.
[16] D.A. Durden, P. Kebarle, A. Good, J. Chem. Phys. 50 (1969) 805.
[17] A. Good, D.A. Durden, P. Kebarle, J. Chem. Phys. 52 (1970) 222.
[18] V.L. Talroze, A.K. Lubimova, Dokl. Acad. Nauk. USSR 86 (1952) 909.
[19] D.P. Stevenson, D.O. Schissler, J. Chem. Phys. 23 (1955) 1353.
[20] F.H. Field, J.L. Franklin, F.W. Lampe, J. Am. Chem. Soc. 79 (1957) 2419.
[21] P.F. Knewstubb, A.W. Tickner, J. Chem. Phys. 38 (1963) 464.
[22] P. Kebarle, in Techniques for the Study of Ion-molecule Reactions, J.M. Farrar and W. Saunders (Eds.), John Wiley, New York (1988) p. 221.
[23] F.J. Garrick, Phil. Mag. 9 (1930) 131.
[24] R.S. Narcisi, A.D. Bailey, J. Geophys. Res. 70 (1965) 3787.
[25] F. Fehsenfeld, A.L. Schmeldekopf, E.E. Ferguson, J. Chem. Phys. 46 (1967) 2802.

[26] F. Fehsenfeld, E.E. Ferguson, J. Geophys. Res. 74 (1969) 2217.
[27] J.L. Beauchamp, Ann. Rev. Phys. Chem. 22 (1971) 527.
[28] D. Van Raalte, A.G. Harrison, Can. J. Chem. 41 (1963) 3118.
[29] J.P. Briggs, R. Yamdagri, P. Kebarle, J. Am. Chem. Soc. 94 (1972) 5128.
[30] P. Kebarle, J. Am. Chen. Soc. 95 (1973) 3504.
[31] M.T. Bowers, D.H. Aue, H.M. Webb, R.T. McIver, J. Am. Chem. Soc. 93 (1971) 4314.
[32] R.T. McIver, Rev. Sci. Instrum. 41 (1970) 555.
[33] T.B. McMahon, J.L. Beauchamp, Rev. Sci. Instrum. 43 (1972) 509.
[34] D.H. Aue, M.T. Bowers, in Gas Phase Ion Chemistry, Vol. 2, M.T. Bowers (Ed.), Academic Press, New York, 1979.
[35] D.K. Bohme, G.I. McKay, H.I. Schiff, J. Chem. Phys. 73 (1980) 4976.
[36] K. Tanaka, G.I. McKay, D.K. Bohme, Can. J. Chem. 56 (1978) 193.
[37] R. Yamdagni, P. Kebarle, J. Am. Chem. Soc. 98 (1976), 1320.
[38] Y. Lau, P. Kebarle, J. Am. Chem. Soc. 98 (1976) 7452.
[39] T.B. McMahon, P. Kebarle, J. Am. Chem Soc. 107 (1980) 2612.
[40] J.F. Wolf, S.R.H. Staley, I. Koppel, M. Taagepera, R.T. McIver, J.L. Beauchamp, R.W. Taft, J. Am. Chem. Soc. 99 (1977) 5417.
[41] R.W. Taft, J.F. Wolf, J.L. Beauchamp, G. Scorrano, E.M. Arnett, J. Am. Chem. Soc. 100 (1970) 1240.
[42] Y.K. Lau, K. Nishizawa, A. Tse, R.S. Brown, P. Kebarle, J. Am. Chem. Soc. 103 (1981) 6291.
[43] Y.K. Lau, P.P. Saluja, P. Kebarle, R.W. Alder, J. Am. Chem. Soc. 100 (1978) 7328.
[44] J.E. Szulejko, T.B. McMahon, J. Am. Chem. Soc. 115 (1993) 7839.
[45] R. Yamdagni, P. Kebarle, J. Am. Chem. Soc. 95 (1973) 4050.
[46] K. Hiraoka, R. Yamdagni, P. Kebarle, J. Am. Chem. Soc. 95 (1973) 6833.
[47] R. Yamdagni, P. Kebarle, Can. J. Chem. 52 (1974) 861.
[48] R. Yamdagni, T.B. McMahon, P. Kebarle, J. Am. Chem. Soc. 96 (1974) 4035.
[49] J.B. Cumming, P. Kebarle, Can. J. Chem. 56 (1978) 1.
[50] J.B. Cumming, P. Kebarle, J. Am. Chem. Soc. 100 (1978) 1835.
[51] J.E. Bartmess, R.T. McIver, J.S. Miller, J. Am. Chem. Soc. 101 (1979) 6046.
[52] J.E. Bartmess, R.T. McIver, in Gas Phase Ion Chemistry, M.T. Bowers Ed., Vol. 2, Academic Press, New York, 1979.
[53] J.E. Bartmess, J.A. Scott, R.T. McIver, J. Am. Chem. Soc. 101 (1979) 6046.
[54] J.E. Bartmess, J.A. Scott, R.T. McIver, J. Am. Chem. Soc. 101 (1979) 6056.
[55] A.B. Viggiano, M.J. Henchman, F. Dale, C.A. Deakine, J.F. Paulson, J. Am. Chem. Soc. 114 (1992) 4299.
[56] E.P. Hunter, S.G. Lias, J. Phys. Chem. Ref. Data 27 (1998) 3.
[57] J.E. Bartmess, NIST Chemistry WebBook, NIST Standard Reference Database Number 69, W.G. Mallard, P.J. Lindstrom (Eds.), NIST, Gaithersburg, MD, 2000.
[58] E.M. Arnett, F.J. Mones III, M. Taagepera, W.G. Henderson, J.L. Beauchamp, D. Holtz, R.W. Taft, J. Am. Chem. Soc. 94 (1972) 4724.
[59] J.J. Solomon, F.H. Field, J. Am. Chem. Soc. 97 (1975) 2624.
[60] J.J. Solomon, F.H. Field, J. Am. Chem. Soc. 98 (1976) 1567.
[61] M. Meot-Ner, J.J. Solomon, F.H. Field, J. Am. Chem. Soc. 98 (1976) 1025.
[62] M. Meot-Ner, F.H. Field, J. Chem. Phys. 64 (1976) 277.
[63] R.B. Sharma, D.K. Sen Sharma, K. Hiraoka, P. Kebarle, J. Am. Chem. Soc. 107 (1985) 3747.
[64] H.C. Brown, Acc. Chem. Res. 16 (1983) 432.
[65] G.A. Olah, G.K.S. Pankash, M. Saunders, Acc. Chem. Res. 16 (1983) 440.
[66] C. Walling, Acc. Chem. Res. 16, (1983) 448.
[67] C.A. Grob, Acc. Chem. Res. 16 (1983) 455.
[68] R.H. Staley, R.D. Wieting, J.L. Beauchamp, J. Am. Chem. Soc. 99 (1997) 5964.
[69] P.P.S. Saluja, P. Kebarle, J. Am. Chem. Soc. 101 (1979) 1084.
[70] D. Holtz, J.L. Beauchamp, S.D. Woodgate, J. Am. Chem. Soc. 92 (1970) 7484.
[71] T.B. McMahon, T. Heinis, G. Nicol, J.E. Hovey, P. Kebarle, J. Am. Chem. Soc. 110 (1988) 7591.
[72] N.G Adams, D. Smith, Chem. Phys. Lett. 79 (1981) 563.
[73] D. Smith, N.G. Adams, Astrophys. J. L87 (1978) 220.
[74] J.T. Keating, P.S. Skell, in Carbonium Ions, Vol. II, G. Olah, P.V. Schleyer (Eds.), Wiley Interscience New York, 1970.
[75] G.P. Ford, J.D. Scribner, J. Am. Chem. Soc. 103 (1983) 349.
[76] N.M. Gluhorster, J.E. Szulejko, T.B. McMahon, J.D. Gaud, A.P. Scott, .J. Smith, A. Pross, L. Radom, J. Phys. Chem. 98 (1994) 13099.
[77] A.G. Harrison, Chemical Ionization Mass Spectrometry, CRC Press, Boca Raton, Florida.
[78] F.C. Fehsenfeld, A.L. Schmellekopf, H.I. Schiff, E.E. Ferguson, Plan. Space Sci. 15 (1967) 373.
[79] L.B. Loeb, in Gaseous Electrons, University of California Press, Berkeley, 1961, p. 375.
[80] J.E. Lovelock, Anal. Hem. 35 (1963) 474.
[81] W.E. Wentworth, E.C.M. Chen, J. Chromatogr. 186 (1979) 99.
[82] L. Eberson, Adv. Free Radical Biol. Med. 1 (1975) 19.
[83] P.R. Rich, Farad. Disc. Chem. Soc. 74 (1982) 3183.
[84] R.D. Mead, A.E. Stevens, W.C. Lineberger, in Gas Phase Ion Chemistry, Vol. 3, M.T. Bowers (Ed.), Academic Press, New York, 1984, p. 214.
[85] P.S. Drazaic, J. Marks, J.T. Brauman, in Gas Phase Ion Chemistry, Vol. 3, M.T. Bowers (Ed.), Academic Press, New York, 1984, p. 168.
[86] E.K. Fukuda, R.T. McIver, J. Chem. Phys. 77 (1982) 4942.
[87] E.K. Fukuda, R.T. McIver, J. Phys. Chem. 87 (1983) 2993.
[88] G. Caldwell, P. Kebarle, J. Chem. Phys. 80 (1984) 577.
[89] E.P. Grimsrud, G. Caldwell, S. Chowdhury, P. Kebarle, J. Am. Chem. Soc. 107 (1985) 4627.
[90] P. Kebarle, S. Chowdhury, Chem. Rev. 87 (1987) 513.
[91] P. Kebarle, Ann. Rev. Phys. Chem. 28 (1977) 445.

[92] R.G. Keesee, A.W. Castleman, Jr., J. Phys. Chem. Ref. Data 15 (1986) 1011.
[93] M.M. Meot-Ner (Mautner), S.G. Lias, NIST Chemistry WebBook, NIST Standard Reference Database Number 69. W.G. Mallard, P.J. Lindstrom (Eds.), NIST, Gaithersburg, MD (2000) (http://webbook.nist.gov).
[94] Y. Marcus, Ion Solvation, John Wiley, Chichester, 1985, p. 105.
[95] T.F. Magnera, G. Caldwell, J. Sunner, S. Ikuta, P. Kebarle, J. Am. Chem. Soc. 69 (1984) 1.
[96] K. Hirao, P. Kebarle, Can. J. Chem. 67 (1989) 1261.
[97] P. Kebarle, G.W. Dillow, K. Hirao, S. Chowdhury, Farad. Discuss. Chem. Soc. 85 (1988) 23.
[98] W.P. Kraemer, G.H.F. Diercksen, Theoret. Chim. Acta (Berlin) 27 (1972) 265.
[99] W.P. Kraemer, G.H.F. Diercksen, Chem. Phys. Lett. 6 (1970) 463.
[100] G.H.F. Diercksen, W.P.R. Kraemer, Theoret. Chim. Acta 23 (1972) 387.
[101] M.D. Newton, S. Ehrenson, J. Am. Chem. Soc. 93 (1971) 4971.
[102] M.D. Newton, J. Chem. Phys. 67 (1977) 5636.
[103] E. Clementi, H. Popkie, J. Chem. Phys. 57 (1972) 107.
[104] H. Kistenmacher, H. Popkie, E. Clementi, J. Chem. Phys. 58 (1973) 1689.
[105] M.H. Mruzik, F.F. Abraham, D.E. Schreiber, G.M. Pound, J. Chem. Phys. 64 (1976) 481.
[106] F.F. Abraham, M.R. Mruzik, Faraday Dis. Chem. Soc. 61 (1976) 36.
[107] G. Corngiu, E. Clementi, E. Pretch, W. Simon, J. Chem. Phys. 70 (1979) 1288.
[108] J. Chandrasekar, D.C. Spellmayer, W.L. Jorgenson, J. Am. Chem. Soc. 106 (1984) 903.
[109] S.K. Spears, F.C. Fehsenfeld, J. Chem. Phys. 56 (1972) 5698.
[110] M. Yamashita, J.B. Fenn, J. Phys. Chem. 88 (1984) 4451.
[111] J.B. Fenn, M. Mann, C.K. Menz, S.F. Wong, C.M. Whitehouse, Science 246 (1985) 64.
[112] A.T. Blades, P. Jayaweera, M.G. Ikonomou, P. Kebarle, J. Chem. Phys. 92 (1990) 5900.
[113] J.S. Klassen, Y. Ho, A.T. Blades, P. Kebarle, in Advances in Gas Phse Ion Chemistry, Vol. 3, N.G. Adams, L.M. Babcock (Eds.), JAI Press, London, England 1998, p. 255.
[114] A.T. Blades, J.S. Klassen, P. Kebarle, J. Am. Chem. Soc. 118 (1996) 12437.
[115] H. Deng, P. Kebarle, J. Am. Chem. Soc. 120 (1998) 2925.
[116] M. Peschke, A.T. Blades, P. Kebarle, J. Am. Chem. Soc. 122 (2000) 1492.
[117] R.D. Smith, J.A. Loo, L. Ogorzalek, R.R. Loo, M. Busman, H.R. Udseth Mass Spectrom. Rev. 10 (1991) 359.
[118] J. Wu, C.B. Lebrilla, J. Am. Chem. Soc. 115 (1993) 3270.
[119] Z. Wu, C. Fenselau, J. Am. Chem. Soc. Mass Spectrom. 6 (1995) 91.
[120] P.D. Schnier, D.S. Gross, E.R. Williams, J. Am. Chem. Soc. Mass Spectrom. 6 (1997) 1086.